University of Stavanger

FACULTY OF SCIENCE AND TECHNOLOGY

MASTER'S THESIS

Study programme/specialisation: Master of Science in Petroleum Engineering Specialization- Natural Gas Engineering	Spring semester, 2021 Open access

Author: Gunel Ismayilova

Supervisor(s): Prof. Rune Wiggo Time

Sr.Eng. Andrianifaliana Herimonja Rabenjafimanantsoa

Vineet Vishnu Mukim

Title of master's thesis:

"Influence of density, viscosity and interfacial tension on liquid droplet dynamics from an open-ended vertical capillary pipe. An experimental investigation."

Credits: 30 ECTS

Keywords: Surface Tension Air-drag Force Image Processing Droplet shape	Number of pages: 66 Stavanger, 15th June 2021

Abstract

The principal objective of the present work is to measure the surface tension of liquids by using a drop weight method by adding new techniques to measure exact drop size and shape, which is linked to the fall velocity and the air drag forces. This thesis is purely experimental. The measurement of the surface tension by Drop weight Method can be implemented with essential laboratory equipment on its most straightforward configuration, but if a detailed analysis is desired can also be implemented with more advanced equipment to see what is involved inside the experiment, this also implies a higher level of complexity on data processing and understanding of the results. In order to test the method, it was decided to use fluids that can be easily found in the laboratory and within the most extensive possible range.

The principle of this method is to use burette radius for the droplet size as a reference and use drop weight as the most direct measure. While droplet can have different size, shape and air resistance, drop mass is constant. In addition to that, not only the surface tension was measured, but also the Python OpenCV library was used to analyze the shape of the matrix, how droplets are formed on the tip of the burette and the diameter of each droplet via slow-motion video frames. Once the data acquired, the surface tension was attempted to be calculated by exact droplet sizes.

The associated error to the calculations is no larger than 1.92 %. Finally, the possible reasons for these errors are briefly discussed.

Acknowledgement

First of all, I would like to thank UiS, which gave me the chance to write the experimental thesis that I got much voluble knowledge and experience from this work. The present work was written as part of the completion of a master program to obtain the Degree of MSc in Petroleum Engineering with specialization in Natural Gas Technology.

I would like to express my gratitude to my supervisor, Professor Rune Wiggo Time, for his overall guidance, ideas, and support in theoretical questions, as well as explaining the logic and insights of image processing coding throughout this work. He is an inexhaustible source of good ideas and a thoughtful mentor.

I am also grateful to Senior Engineer Herimonja A. Rabenjafimanantsoa for his help in assembling the equipment and his endless support in software parts and writing parts, and for pushing me every day to fulfil this work.

I wish to thank my co-supervisor, Vineet Vishnu Mukim, for his generous help, time and for always making me think about the logic behind the theories.

This thesis was not as nearly as possible without their great contribution.

I wish to appreciate all my friends at UİS who spent three incredible years in Stavanger and contributed to my growth as a person.

Last but not least, my master program could not have been completed without the unconditional love and support of my family and especially my mum. No words describe my appreciation for their support and love for me.

Table of Contents

List of Figures

List of Tables

Nomenclature

Abbreviations

SI	International system of units
Fps	Frames per second
ρ	Density
m	Mass
v	Volume
γ	Surface tension
μ	Viscosity
τ	Shear stress
F_D	Air-drag force
F	Correction factor for Tata's `Law

Chapter 1 Introduction

Physical qualities such as density, viscosity, surface tension are important in research and industry. When it comes to small-scale processes, surface tension can be said to play a significant role.

Several examples can be given: all the small living creatures live in an environment mainly dominated by surface tension, some animals and plants have developed natural strategies for water-repellency, dynamics of magma chambers and volcanoes, the dynamics of raindrops and their role in the biosphere, the design of ways to coat the insects and leave the plant unharmed in the fight against plagues, application of cavitation in medicine to treat tumours and kidney stones, coating technology to repel dust and water, among others [1].

Inside the Petroleum Industry, there are many fields where surface tension plays an important role. Inside the pore space on the reservoir rocks, the distribution and the flow of the fluids is highly influenced by the wettability of the rock, a property directly related to the surface tension. In addition, during the good drilling process and workover operations, it is essential to use an appropriate fluid. The use of surfactants that modifies the surface tension is widespread. By understanding the way these fluids interact with the reservoir rock in the zone close to the wellbore is a key factor for the success of an operation. Otherwise, the pore space can be clogged and left the well with limited or no productivity. Conversely, a proper comprehension of the fluid properties at downhole conditions and how they interact with other fluids will result in a successful job.

As a preparation for this thesis to obtain background knowledge and improve the understanding of all the variables involved in this experiment, there were read some articles about experiments for the determination of the surface tension, some of them with very basic theory and knowledge about what it is involved in the process of the measurement using this method, and other recent articles with more advanced techniques. Much has been said in these documents and publications by the use of basic laboratory equipment for acquiring the data that somehow limited the capacity of the analysis. By the use most recent technology in data acquisition, it can be understood in a better way all the variables involved in the process of determining the surface tension. This motivates to analyze these aspects by using state-of-the-art equipment: High-resolution slow-motion cameras, digital image processing, among others. Since the

formation and falling of a droplet take milliseconds, the use of the techniques previously mentioned will help perform the measurement of the surface tension and analyze and describe the phenomena and peculiarities around this experiment. To perform adequate processing of the measurements obtained from the experiment, it is recommended the use of Python or other coding tools. Code can be developed to perform proper image analysis.

1.2 Objective

The objective of this project is to build a system to calculate the surface tension and analyze droplet during the vertical fall. Several tasks of the project can be specified as follows:

1. To study fluid dynamics and drop weight method;
2. To study air-drag force during the vertical fall;
3. To develop a corresponding setup in the laboratory;
4. To analyze droplet weight, velocity and calculate surface tension for different liquids;
5. To analyze droplet shape during the fall by image processing.

1.3 Outline of the Thesis

The thesis is experimental and aims to investigate droplet fall through the open-ended vertical pipe and find out the surface tension for different liquids and analyze droplet shape through the fall.

The theoretical concept of fluid dynamics is described in Chapter 2. Also, several parameters are briefly discussed.

The detailed description of the Drop weight method is described in Chapter 3. The correction factor explanations are put here as well.

Chapter 4 shows the experimentation part. The scheme of setup, all equipment and their working principle is demonstrated in Chapter 4. In addition to that visualizing tools, and high-speed recording part is shown here.

Chapter 5 consists of results and discussions for surface tension calculations with possible errors, droplet shape deformations and also air drag force effects.

Conclusion and some ideas for further work are addressed in Chapter 6.

All the codes are used during the analyses, the picture of the setup and PASCO Capstone testing results for different experiments are demonstrated in the Appendix part.

Chapter 2 Theory

2.1 Fluid Dynamics

Fluid dynamics is a branch of physics that alludes to fluid flow, including interactions as two fluids contact each other. In this field of context, either liquid or gas is considered as a "fluid" [2].

Fluid dynamics is a subdiscipline of fluid mechanics (another subdiscipline is fluid statistics which refers to a static state of fluid)that deals with fluid in a motion has an essential wide range of applications such as analyzing ocean waves, blood circulation, determining the forces and moments on aircraft, calculating mass flow rate in an oil pipeline [3]. Wind turbines, rocket engines, and oil pipeline are the main technological applications of fluid dynamics [3].

2.2 Density

A material's density is a measure of mass per unit volume. In a nutshell, density is a measurement of how tightly matter is crammed together. Archimedes, a Greek scientist, discovered the density principle [4]. To calculate the density (usually represented by "ρ") of an object, take the mass (m) and divide by the volume (v):

$$\rho = \mathrm{m}/v \tag{2.1}$$

The SI unit of density is kilogram per cubic meter (kg/m^3). The cgs unit of grams per cubic centimetre (g/cm^3) is also prevalent [4].

2.3 Viscosity

Viscosity is the internal friction due to molecular cohesion in fluids, which results in resistance to flow, and low viscosity means that it is easy to flow [5].

It is a critical property affecting the fluidity of the liquid. It is measured in poise (P), 0.100 kg m^{-1} s^{-1}, but usually expressed as centipoise (cP), 0.001 kg m^{-1} s^{-1}. For a frame of reference, the viscosity of some common materials is as follows: water ~one cP, olive oil ~80 cP, honey 2000–10,000 cP, peanut butter ~250,000 cP, and chocolate ~1,000,000 cP.

2.4 Surface Tension and Interfacial Tension

Surface tension is a measure of cohesive forces between liquid molecules presented at the surface [6]. Obviously, surface tension and molecular structure are related to each other, but no quantitative observations have been acquired [5].

.

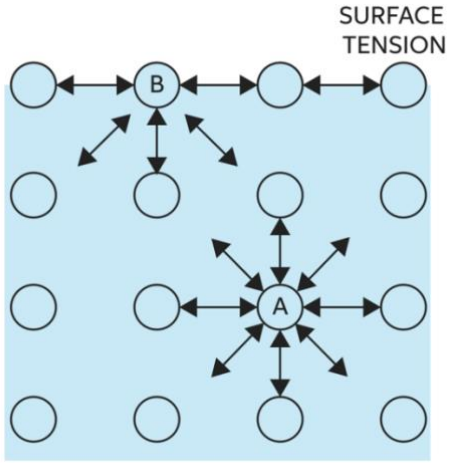

Figure 2.1: Cohesive forces among liquid molecules explaining the origin of the surface tension at the liquid-gas interface [7].

It can be explained that liquid molecules are attracted to each other on a molecular scale. These are subject to strong, attractive forces exerted by other molecules in their vicinity at the surface. The result of these attractive forces acts in a plane that is tangent to the surface at a particular point. The magnitude of this resultant force acting perpendicular to a line of unit length in the surface is known as surface tension [8].

Another physically appealing definition is that a certain amount of energy is required to reach below the free surface of a liquid and pull molecules upward to the surface to form a new area. The energy required per unit area formed is described as surface tension [9].

Surface tension can also be defined as energy/area and has the units of force/length: J/m= N/m.

Surface tension refers to the elastic tendency of a fluid surface, which makes it acquire the least possible surface area. In general, it is surface energy that is minimized in view of external forces. But under static conditions, this is mainly equivalent to minimizing the area. At liquid-air interfaces, surface tension results from the greater attraction of liquid molecules to each other (cohesion) than to the molecules in the air (adhesion). The overall effect can be explained by that an inward force at the liquid surface that causes the liquid to behave as if the surface were covered with an elastic membrane. Because of the relatively high attraction of water molecules for each other, water has a higher surface tension (72.8 mN/m at 20°C, 68°F) compared to many other liquids [10].

Thus, the surface tension indicates cohesive forces between molecules at the surface; here, the "surface" term must be defined more clearly. Suppose the boundary ("surface") is between a liquid and a solid or between a liquid and a gas (air) phases. In that case, the attractive forces are, in this case, referred to as surface tension, but the attractive forces between two immiscible liquids are referred to as interfacial tension [11].

Interfacial tension is somewhat similar to surface tension insofar as cohesive forces are also involved. However, Interfacial tension is the force of attraction between molecules at the interface of two fluids. The interaction occurs at the surfaces of the substances involved, that is, at the interface [12].

In SI units for interfacial tension are milli-Newtons per meter (mN/m). These are equivalent to the former units of dynes per centimeter (dyne/cm) [13].

Significance

The interfacial tension has a significant role in many processes and phenomena where different phases touch one another:

1. *Emulsions and emulsifiability***:** The interfacial tension affects the tendency for the phases to separate and the emulsifiability [14].

2. *Flooding (for example, with tertiary crude oil production):* If the interfacial tension is reduced through surfactants, the organic phase can be mobilized after flooding with water.
3. *Quality tests of hydrophobic liquids:* The ageing of a hydrophobic liquid often goes hand in hand with a reduction in the interfacial tension with water. In such cases, measurement of the interfacial tension is a critical quality test, for example, with transformer oil.
4. In the case of solid-liquid phase boundaries, the interfacial tension affects the long-term stability of the interface contact, for example, with glueing and coating processes.

2.4.1 Measuring Methods

Liquid-liquid interface:

1. Ring method according to Du Noüy: The force acting on an optimally wettable ring as a result of the tension of the withdrawn liquid lamella when moving the ring from one phase to another is measured in this method [15].
2. Plate method according to Wilhelmy: The force acting on an optimally wettable plate that is immersed vertically in the lower phase is measured in this method.
3. Rod method: As the plate method, wherein a cylindrical rod with a smaller wetted length is used for measurement with a smaller liquid volume.
4. Drop volume method: The volume of a drop of liquid produced at a vertical capillary in another liquid is measured at the moment of its detachment.
5. Spinning drop method: A horizontal capillary filled with a bulk phase and a drop phase is set in rotation. The diameter of the drop, which is elongated by centrifugal force, correlates with the interfacial tension.
6. Pendant drop method: The shape of a drop on a needle in a bulk liquid phase is determined, among other things, by the interfacial tension. The interfacial tension can be ascertained from the image of the drop using drop shape analysis.

Liquid-solid interface:

1. Measurement of the contact angle: As well as its surface free energy, the interfacial tension of a solid with particular liquids can also be calculated from the contact angle of the various liquids with the solid [16].

2.5 Fluids

2.5.1 Newtonian Fluids

A Newtonian fluid is a fluid that exhibits a linear relation between the applied shear stress τ and the shear rate γ. The relation is given by:

$$\tau = \mu\gamma \tag{2.2}$$

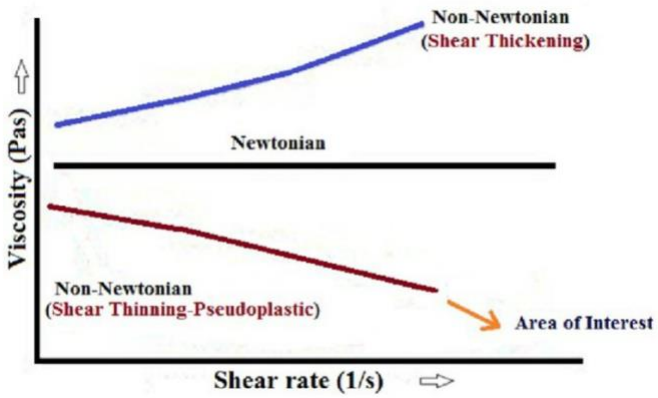

Figure 2.2: Typical rheogram of Newtonian and non-Newtonian fluids [17].

Where the proportionally constant μ is the viscosity of the fluid, a representation of this relation can be found as the black curve in Figure 2.2. In Newtonian fluids, the viscosity is only temperature and pressure-dependent [18]. In this thesis, three fluids were analyzed; all of them are Newtonian fluids to simplify the calculations and applicability of the methods.

2.5.2 Non-Newtonian Fluids

A non-Newtonian fluid is a fluid that exhibits a non-linear relation between the applied shear stress, τ and the shear rate γ. In non-Newtonian fluids, the viscosity, in addition to temperature and pressure, is shear stress and shear rate dependent [17].
There are mainly three types of non-Newtonian fluids. Figure 2.2 shows the comparison between these fluids relative to a Newtonian fluid.

1. Plastic: Shear-thinning fluids, which means that the viscosity decreases as the shear rate increases.
2. Pseudoplastic: Also, shear-thinning fluids, but the transition between plastic and pseudoplastic can be hard to distinguish.
3. Dilatant: Shear-thickening fluids, which means the viscosity increases as the shear rate increases

The plan was to test non-Newtonian liquids also. However, there was not enough time to do well-qualified experiments. It is time-consuming to prepare homogeneous fluids without small air bubbles. Bubbles would severely impact also the surface tension.

2.6 Air Drag Forces of the Falling Drop

Two external forces are acting on an object as it falls through the atmosphere. The first force is the gravitational force, expressed as the weight of the object, and the second force is the aerodynamic drag of the object. At speeds less than about 1 m/s, the drag force on a sphere is proportional to the speed, and it is given by Stokes' law. At higher speeds, the drag force is proportional to the velocity squared and is usually small compared with the gravitational force if the object mass is large and its speed is low [19].

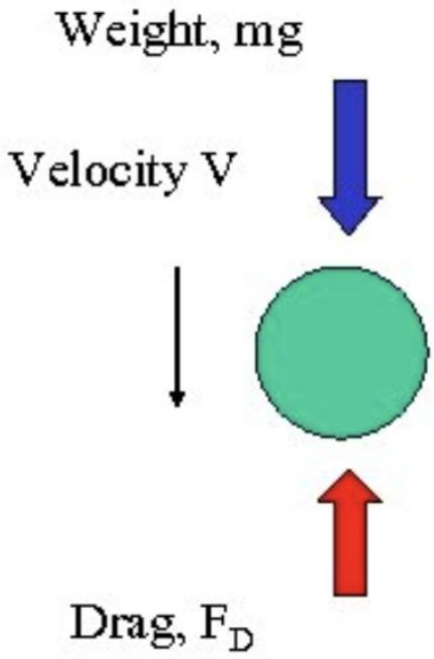

Figure 2.3: Forces that affect a falling droplet on the air

The equation of motion for a droplet of mass m falling vertically at speed v is given by equation 2.3 :

$$m\frac{dv}{dt} = mg - F_{\mathrm{D}} \tag{2.3}$$

and the drag force is:

$$F_{\mathrm{D}} = 0.5C_{\mathrm{D}}\rho A v^2 \tag{2.4}$$

Where C_D is the drag coefficient, ρ is the fluid density, and $A = \pi D^2/4$ is the cross-sectional area of the falling drop.

In other words, as droplets fall, air resists their downward motion, and the amount of this air resistance is based on the size of the drop and its rate of fall or velocity. The speed of the falling droplet increases until the air resistance equals the downward pull of gravity and then begins to fall at a constant speed, no longer accelerating downward. This constant speed that is finally reached is called the drop's terminal velocity or fall speed.

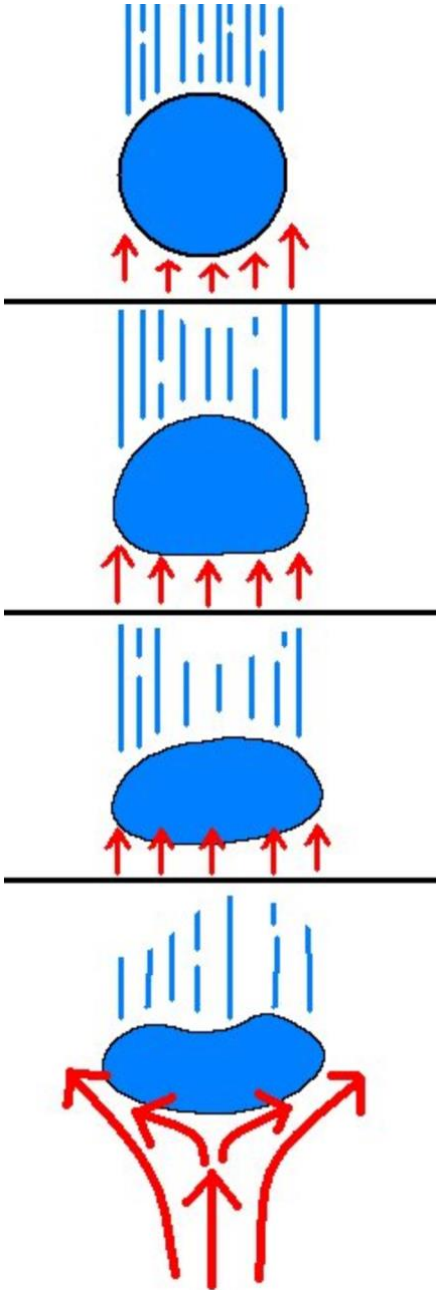

Figure 2.4: Shape deformation of the droplet during the fall

Chapter 3
Drop Weight Method

It is one of the standard methods to measure surface and interfacial tension. As mentioned before, the surface and interfacial tension are essential parameters for fluids; they determine the quality of many industrial products such as coatings, cosmetics, jet printing, detergents, lubricants, pharmaceuticals, pesticides, food products and agrochemicals. Additionally, interfacial tension significantly affects other chemical procedures such as catalysis, adsorption, distillation, and extraction phenomena.

Some important factors need to be considered while using the drop weight method to determine surface tension.

3.1 Determining Parameters

3.1.1 Operation Mode.

There are three operational modes for drop weight experiment: *static, dynamic, and quasi-static*.

The static mode is operated by a relatively slow rate of drop formation. Usually, the surface tension of pure liquids is measured by this model. To measure the static surface tension, the weight or volume of the detached drop is measured after a certain period of drop formation time.

Secondly, in the dynamic mode, measurements are done under a constant droplet formation flow rate. Instead of drop weight, the volume of each detached drop is determined at every time interval. The dynamic mode is prevalent for dilute solutions, which contains surface-active agents (e.g., surfactants) [20] [21].

Similarly, the quasi-static mode also determines dynamic surface tension, however, a smaller time interval than the dynamic model. It consists of growing a drop of a defined volume at a dripping tip in the possible minimum formation time. As an example, surface tension

measurements are done by quasi-static model for slow adsorption kinetic solutions (from a few minutes to a few hours) such as polymer solutions, protein solutions [20].

3.1.2 Drop Number

Generally, many drops are required to determine the average weight of an accumulated liquid per drop in a static mode. Additionally, the first few detached drops are neglected to reduce hydrodynamic effects; from 10 to 30 drop number has been proposed as reliable numbers. Statistically, 30 drops of the sample are quite adequate to have a reproducible and accurate measurement [22] [23].

3.1.3 Evaporation Effect

Possible errors due to the evaporation could be significant for volatile and aqueous solutions during slow drop formation time. Therefore, however, accuracy is very important in some cases to eliminate and minimize evaporation effects; fast drop procedures are preferred. The drops are drawn to nearly full size (about 95%) [24].

3.1.4 Hydrodynamic Effects

The drop weight of a sample differs depending on the drop formation time from a dripping tip, according to the research of Hoorfar (2006). This means that while measuring drop weight, hydrodynamic factors must be taken into account. In a drop formation time interval of 1 to 30 seconds, even a pure liquid exhibits hydrodynamic effects. Thus, to minimize hydrodynamic effects, surface and interfacial tension measurements should be taken for drop times above the 30s.

3.1.5 Dripping Tip

The most important component of a drop weight or drop volume equipment is the dripping tip. It will have a direct impact on the accuracy of liquid and solution surface and interfacial tension measurements.

The dripping tip should be placed perpendicular to the datum line. The slope of the dripping tip was discovered to be a factor in drop weight determination. Depending on whether the drop is hanging ‘‘pendant up", with the heavier fluid within the lighter or vice versa, different outcomes have been reported for liquid-liquid systems. In conclusion, more research is needed to justify the dripping tip's location

3.1.6 Dripping Tip Size

The tip size for an air-liquid system should be chosen so that the $r/V^{1/3}$ value is between 0.65 and 0.95, a region of minimum correction factor boundary$\left(\ \mathrm{F}\left(r/V^{\mathrm{I}/3}\right) \approx 0.60\right)$. T. dripping tip for a liquid-liquid system, however, should be chosen so that $r/V^{1/3}$ ratio is between 0.50 and 0.65.

3.1.7 Dripping Tip Geometry

As shown in Figure 3.1, the geometry of a dripping tip can be divided into two types: capillary tips and sharp-edge tips.

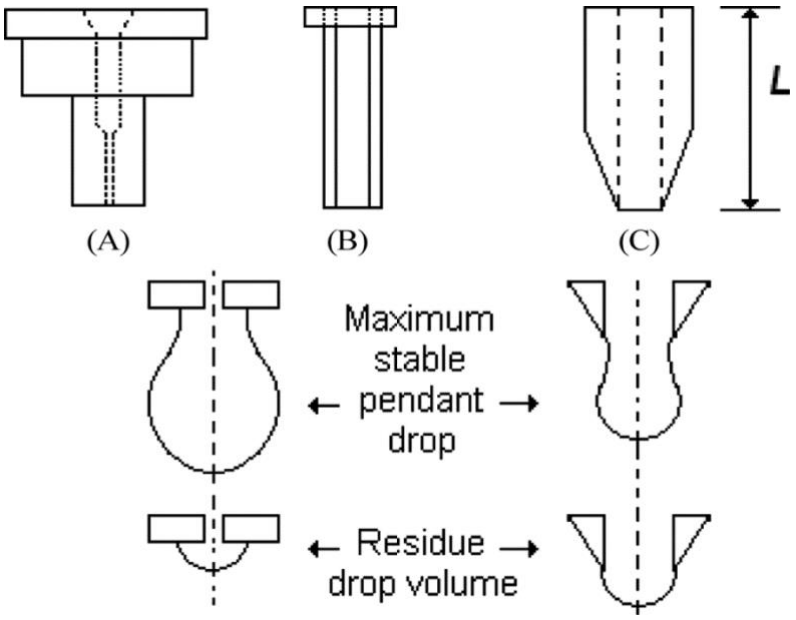

Figure 3.1: (Above) Dripping tip geometry: (A) thick-wall capillary tip, (B) thin-wall capillary tip, (C) sharp-edge tip. (Below) Drop detachment according to the dripping tip geometry.

Therefore, it's very important to record the degree of wetting of the dripping fluid on the surface of the dripping tip; the drops form either at the tip's inner or outer diameter. The inner diameter dimension should be used to calculate surface or interfacial tension. If the drops are formed on the inner diameter and vice versa if the droplets are formed on the outer diameter. And also, drop weight correction factors are different for different dripping tips, which is discussed in further chapters [25].

3.2 The Principle of the Drop Weight Method

Due to the simplicity of handling, easy temperature control, sample size, and good reproducibility, the drop weight method is one of the most preferred surfaces and interfacial tension measurements methods.

This method can be traced back to Tate, who postulated that as the droplet is formed due to the capillary force on the dripping tip, it is gravity that is acting as opposed to it and pulls it down.

Subsequently, Tate's Law states that the drop would fall from the dripping tip when the capillary force is equal to the drop weigh [26].

$$mg = 2\pi r\gamma \tag{3.1}$$

Where m the mass of the droplet, g the acceleration of the gravity is known. The radius of the droplet can also be detected according to the wetting behaviour of the analyzed liquid, and it is accepted either inner or outer radius of the capillary so that this equation γ can be obtained experimentally

Accordingly, Tate's Law can be written as

$$\gamma = mg2\pi r \tag{3.2}$$

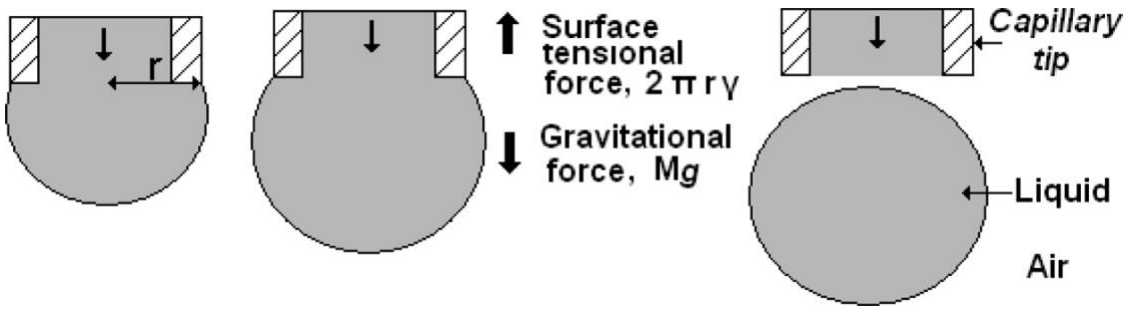

Figure 3.2: Tate's law based forced balance approximation.

Since Tate's law is only a poor approximation and gives underestimated surface tension values. The reason is when the droplet falls, and there is a remaining residue part of the droplet which is not detached from the dripping tip. In practice, to determine the surface tension of the liquid-air interface, some correction factors are needed [24].

Earnshaw presented the most frequently acknowledged correction factor F, which was a combination of experimental data recorded by several other authors, including Harkins and Brown and Wilkinson.[27] The correction factor F is used to correlate the ratio of the real and ideal drop volume to the dimensionless capillary radius $r/V^{1/3}$.

$$F\left(r/V^{1/3}\right) = V/V_{\text{ideal}} \tag{3.3}$$

And the weight of the detached drop is lower than that predicted by equation (3.1), so a correction factor F is added to the original Tate's law,

$$mg = F\gamma 2\pi r \tag{3.4}$$

The mathematical fit presented by Lee–Chan–Pogaku can be used to adjust the experimental values of the correction factor F with high fidelity in the range 0-1.2.[28]

$$\mathrm{F}\left(\frac{r}{V^{\frac{1}{3}}}\right) = 1.000 - 0.9121\mathrm{x}\left(\frac{r}{V^{\frac{1}{3}}}\right) - 2.109\mathrm{x}\left(\frac{r}{V^{\frac{1}{3}}}\right)^2 + 13.38\mathrm{x}\left(\frac{r}{V^{\frac{1}{3}}}\right)^3 - 27.29\mathrm{x}\left(\frac{r}{V^{\frac{1}{3}}}\right)^4 + 27.53\mathrm{x}\left(\frac{r}{V^{\frac{1}{3}}}\right)^5 - 13.58\mathrm{x}\left(\frac{r}{V^{\frac{1}{3}}}\right)^6 + 2.593\mathrm{x}\left(\frac{r}{V^{\frac{1}{3}}}\right)^7 \tag{3.5}$$

Tate's law is recovered in the limit when $r/V^{1/3} << 1$ because the equation above gives F = 1.

When the $r/V^{1/3}$ ratio is between 0.6 and 1, as shown in Figure 3.3, the range of the correction factor values is minimal. Working within this range is thus useful for maximizing the accuracy of experimental outcomes.

It means that, for a given liquid, it's recommended to choose a capillarity size that corresponds to this range of values, as the capillarity tip is so important in drop weight devices.

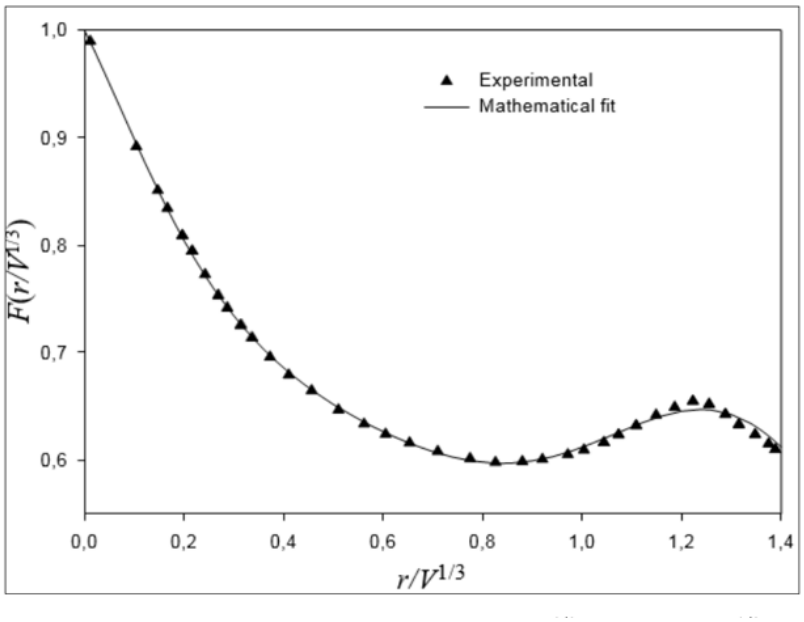

Figure 3.3: Tate's law correction factor $F(r/V^{1/3})$ against $r/V^{1/3}$. Experimental data and mathematical fit according to the equation.

Chapter 4 Experimentation

4.1 Experimental Methodology

The motivation of the following experiment is based on both observing droplet, their's shape and measuring surface tensions and calculating the air drag force for water.

4.2 Experimental Setup

The experiments for surface tension measurements were performed using PASCO equipment at the Mezzanine Laboratory at the University of Stavanger. Once all the equipment elements have been selected, the next step is to continue with the assembly. A diagram of the equipment setup is shown in Figure 4.1. This section will give information about all parts and all equipment for the setup.

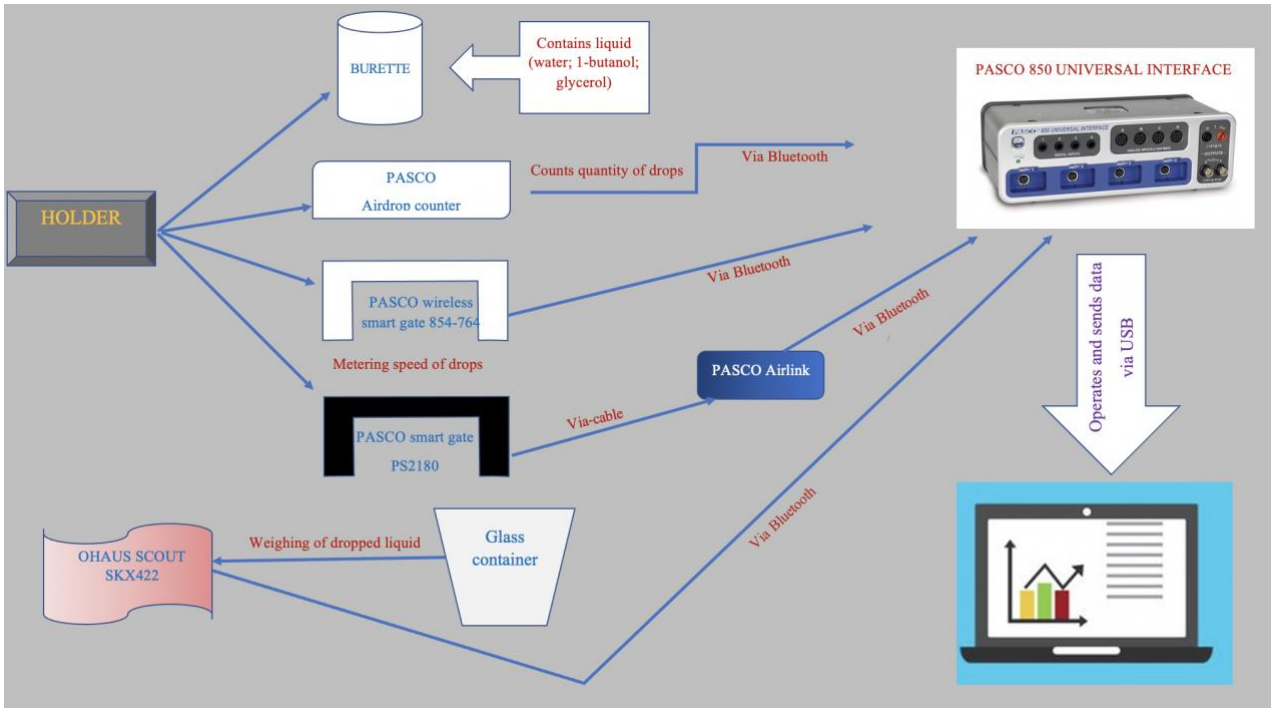

Figure 4.1: Equipment setup

The AutoCAD drawings of the setup are represented in Figure 4.2 below.

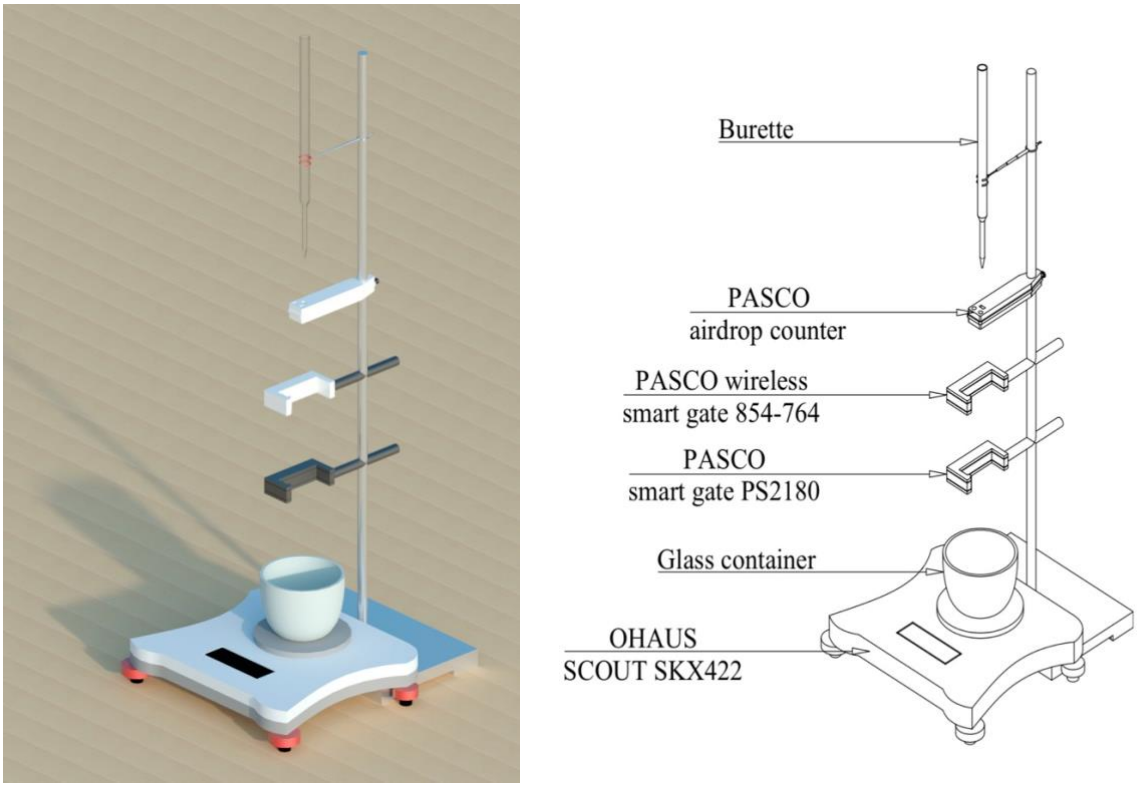

Figure 4.2: 3D and 2D drawings of experimental setup on AutoCAD.

4.2.1. PASCO 850 Universal Interface

PASCO 850 Universal Interface, as seen in Figure 4.3, has been used to have an interface between the computer and other equipment. PASCO Universal Interface is a data acquisition device. It is provided with digital and analogue inputs, can be used simultaneously with other PASPORT interfaces and PASCO Wireless sensors [29]. It is designed specifically to be used in conjunction with PASCO Capstone software that allows the sensors' configuration, displaying the data and analysis of them.

Figure 4.3: PASCO 850 Universal Interface

4.2.2 PASCO Wireless Airdrop Counter

The wireless drop counter with a drop window (18 x 13 mm), which made it easy to align the burette tip with better detection, has been used to count(determine)the number of drops. The counter can detect ten drops per second with drops as small as 0.5 mm.

Figure 4.4: PASCO Wireless drop counter.

4.2.4 PASCO Smart Gates and Airlink

The wireless smart gate 854-764 has been used to measure the velocity of the droplets through the photogate beans. It has dual photogate beams spaced at 1.5 cm to accurately measure speed and velocity [30]. *The smart gate PS2180* is also attached as a 3rd gate (1st is the drop counter, 2nd is the wireless smart gate 857-764). The smart gate PS218 connects directly to any PASPORT interface and has an auxiliary port to daisy chain to an additional photogate [31]. And it is recommended by the smart gate provider to have the measured times relatively long (greater than one-half second) since synchronization is limited to 2ms if two Wireless Smart Gates in the same experiment are used.

Figure 4.5: On the right: Wireless smart gate 854-764; On the left: The smart gate PS218

Pasco Airlink 016-027 interface is connected to the smart gate PS2180 to have a wireless connection with the computer.

Figure 4.6: Pasco Airlink 0160-027

4.2.5 Scale and Burette

OAHUS SCOUT SKX422 (with 0.01g readability) is used to weigh the liquid. The scale has 420 g of maximum capacity [33].

Figure 4.7: On the right: OHAUS SCOUT SKX422.

The calibration was done to ensure the accuracy level of the scale by weight units provided by the University of Stavanger (Figure 4.10). While calibration, an error has been detected and taken into account. As it is seen from Figure 4.8, the scale was weighing extra for 200g and 100g standard weights. So that, an error function of the scale was made on Excel and considered for them (weight) during calculations.

Figure 4.8: Calibration of the scale by standard weights.

The graph below shows the error function of the scale, with regression equal to 1.

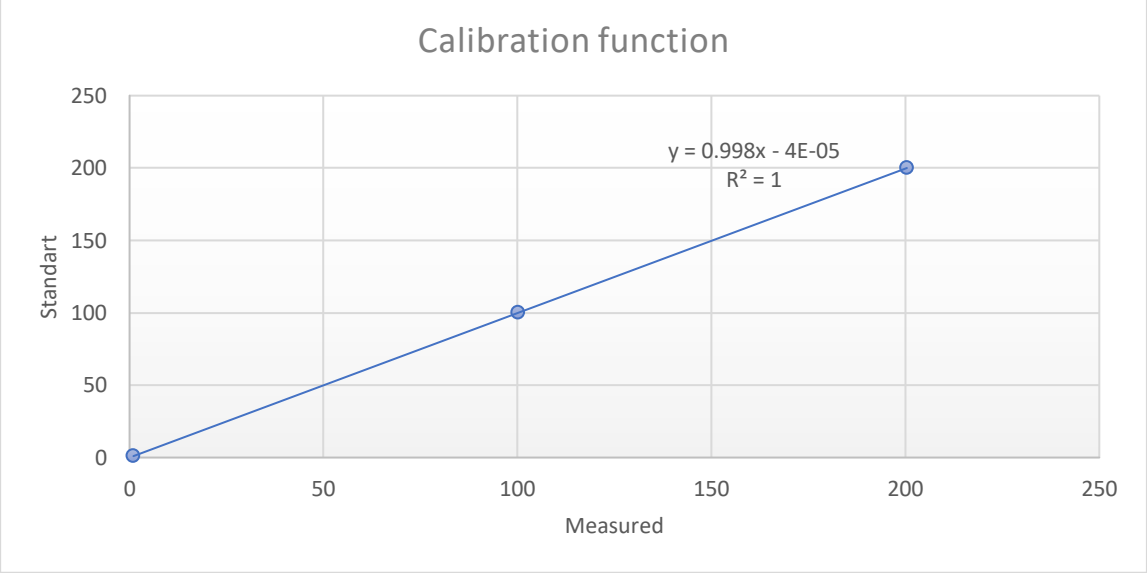

Figure 4.9: The graph of the calibration function of scale.

Figure 4.10: Standard weight provided by the University of Stavanger.

To determine the surface tension by means of the drop weight method, it is required to know the diameter of the dripping tip with high accuracy. Experimental results prove that water, 1-butanol and glycerol drops are formed at the outer perimeter of the dripping tip, so r is the outer radius of the glass capillarity, which was provided by the company as the burette's specification.

Figure 4.11: Burette type and size

In addition to that, a thermometer is used to have an improved accuracy as surface and is dependent on the temperature.

4.2.6 High-speed Recording and Visualization equipment

The surface tension measurements by means of the drop weight method are required to know the diameter of the dripping tip with high accuracy. Experimental results, which have done before, states that water, 1- butanol and glycerol drops are most likely formed at the outer perimeter of the dripping tip. Hence, r is the outer radius of the glass capillarity. The outer diameter of the tip of the burette was known from the specification of the burette. However, actual droplet size and shape were measured, taken with a 12-megapixel iPhone XS camera. In addition to that, to analyze droplet sizes and shapes coming from burette tip slow-motion videos were needed. This camera has 240 fps which was enough to capture droplets with high resolution. Python code was used to separate the video frames to identify sizes and shapes on OpenCV Library.

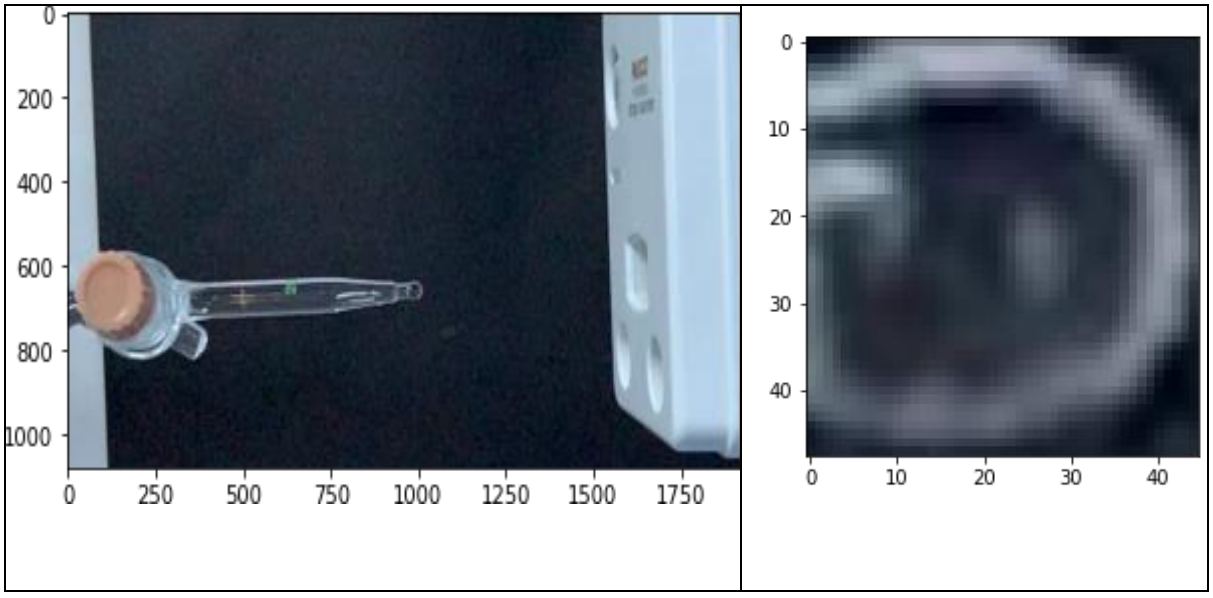

Figure 4.12: Pixel resolution of a droplet on Python.

Slow-motion camera: A BASLER acA800-510uc camera, as seen in, was tested and used to record up to 511 fps with a resolution of up to 800 x 600 pixel (W x H). It could focus objects up to 6 cm, and it was connected to a computer using a USB 3.0 port.

Figure 4.13: Slow-motion camera, BASLER acA800-510uc.

Under testing, it was found that the camera can't record at 500 fps when it is at full resolution even the illumination was not good enough. This problem was fixed by reducing the resolution; however, in this case, droplets were hardly seen (Check Appendix C.4) And that was essential to see droplets to analyze their shape and chaotic movements.

4.2.7 Experimental Procedure

The procedure to determine the surface tension of a given liquid is as follows :

1. The burette was filled with the liquid to be examined and measured at the ambient temperature.
2. To avoid hydrodynamic impacts, the drop formation time was controlled slowly enough. Thirty seconds per drop is sufficient for the liquids studied in this thesis.
3. Thirty drops were fully formed and deposited in a vessel; the first 3-4 droplets were not taken into account in order to eliminate hydrodynamic effects during the drop formation. The weight of the vessel and the radius of the burette tip must be known at this stage (R=1.25 mm). In addition to that, the average diameter of the exact droplets was also measured and applied to the calculations.

In order to be 100% correct, specifications of the burette were asked from the supplier company as well.

4. The vessel in Figure 4.12 containing the 30 drops was weighted with an analytical balance simultaneously, and the average drop weight is calculated.

Figure 4.14: Container

5. The correction factors F was calculated by applying equation (3.5) once the mean drop volume V is calculated from the mean mass m and the density of the liquid, which can be obtained from the technical literature.
6. Finally, the surface tension was calculated by applying the equation (3.4).

The burette in Figure 4.11 above was later filled with water, 1-butanol and glycerol to measure the surface tension of such liquids. Water, 1-butanol and glycerol were used as test samples because they are inexpensive and commercially accessible liquids. It is easy to find data in the bibliography of their physicochemical variables at different temperatures.

4.3 Air Drag force Measurements and Effect.

As mentioned above, the air drag force is important in determining the drag effects on the droplet shape and velocity. In order to identify and analyze that, air drag force was calculated by equation 2.4. Where the air drag coefficient C_{D}, and density ρ were known from the literature and v was measured by two PASCO gates which are shown in Figure 4.4, and as

$A = \pi D^2/4$ is the cross-sectional area of the falling drop, the diameter of the droplet from pixel calculations was used.[34]

Table 4.1: Air drag force measurement

Liquid	Dia**mete**r	Density	Air drag coefficient, C_D	Drop velocity	$\mathbf{F_D}$
	mm	Kg/m^3		m/s	**N**
Water	10	997.05	0.47	1.50	0.42

Chapter 5 Results and Discussions

5.1 Surface Tension Analyzes

This section describes the experimental tests performed to determine the surface tension of the three analyzed liquids, i.e. distilled water, glycerol and 1-butanol. Since the drops formed when applying the drop weight method are not always identical, to calculate the average drop weight, 30 drops were used in each measurement of the three liquids. This procedure also increases the accuracy of this method and ensures reproducibility in measurements. As explained in Chapter, a glass burette was used to determine the surface tension, and three liquids were measured, i.e. distilled water, glycerol and 1-butanol. Table 5.1 shows the main data of the drop weight method obtained.

Table 5.1: Main data of the drop weight method.

Liquid	Outer radius	Density	Drop mass	Drop volume	$r/V^{1/3}$	F
	mm	Kg/m^3	**kg x 10^{-5}**	**m^3 x 10^{-8}**	-	-
Distilled water	1.25	997.05	3.98	3.99	0.36	0.7031
Glycerol	1.25	1258.02	3.57	2.84	0.40	0.6860
1-Butanol	1.25	809.50	1.25	1.	0.50	0.6520

Once the outer tip radius R, the mean drop mass m, and the correction factor F are known, the droplet's surface tension is determined by isolating the surface tension γ from equation (3.4) as below. Note that calculations assume g = 9.80 m/s^2.

5.2 Second Calculation Method

In addition to surface tension calculations in Chapter 5.1, 30 droplet diameters were measured from python code Figure 4.11. An average diameter (D = 11.3 mm) was applied to the Tate Law equation (3.2) to attempt to calculate the surface tension of the water droplet.

Table 5.2: Calculation by exact drop size.

System	Surface tension x 10^{-3} N/m		|Lit. – Exp.|/Lit x 100
	Literature	Experiment	%
Water	71.87	101.32	40.97

5.3 Shape of the Droplet

When the tube radius is small, e.g., R = 0.06 cm, the pendant drop is nearly hemispherical, whereas when the tube radius is large, e.g., R = 0.61 cm, the pendant drop is nearly conical in shape [25]. Thus, the profiles of the pendant drops vary from hemispherical to conical and the contact angle that the pendant drops make with the capillary decrease as capillary radius increases. Thus, there exists the possibility that as R increases, the interface may become flat or even reentrant into the capillary at the contact line. The picture below shows the shape of the sample drop where R = 0.25 cm.

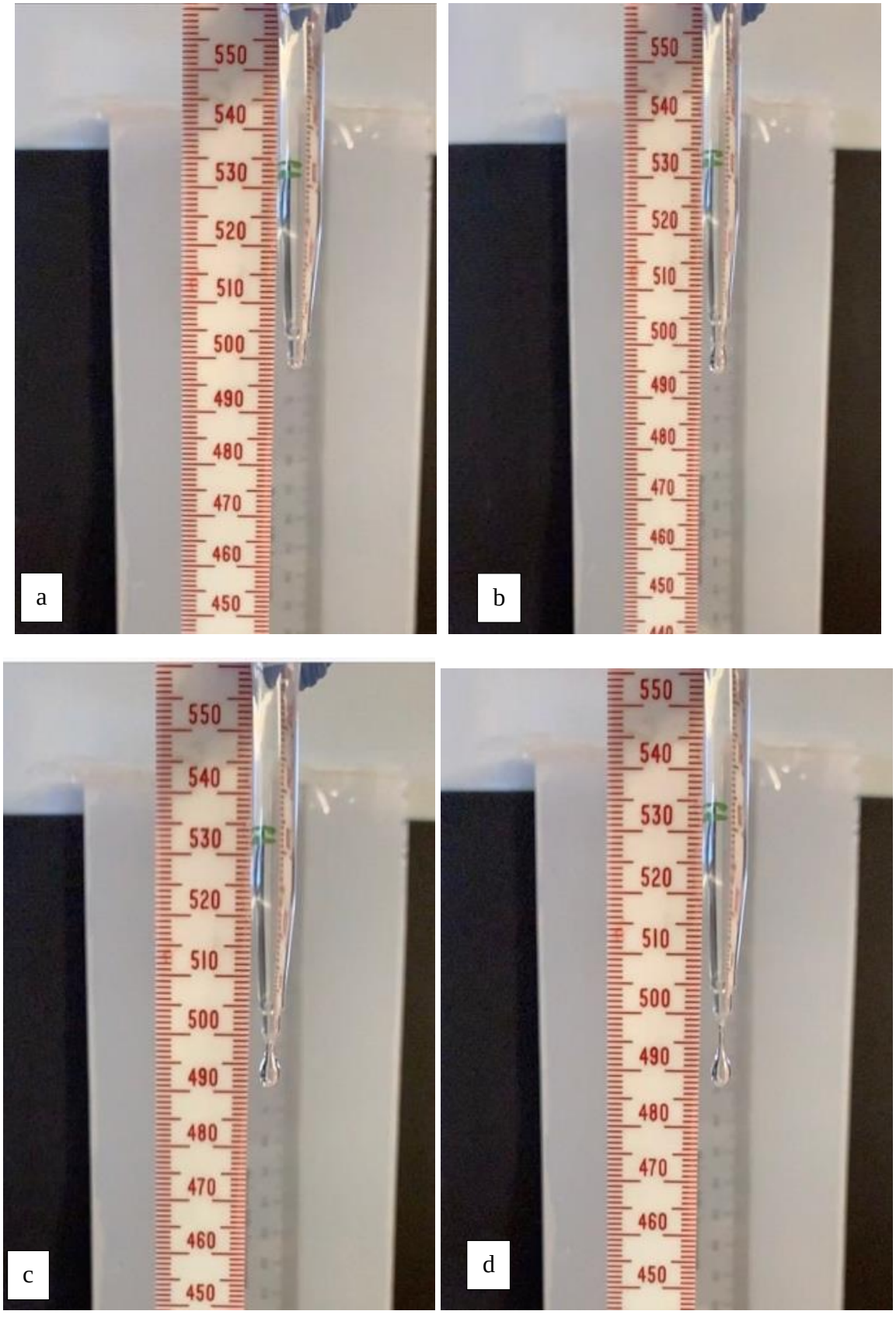

Figure 5.1: Water droplet shape and detachment mechanism.

Figure 5.1 shows the evolution in time of the shape of a drop forming from a capillary of moderate dimensional radius.

Starting from a shape that is a section of a sphere in section a, Figure 5.1 shows that the interface becomes horizontal at the contact line long before pinch-off. That tube invasion can be seen at the incipience of primary drop formation in d.

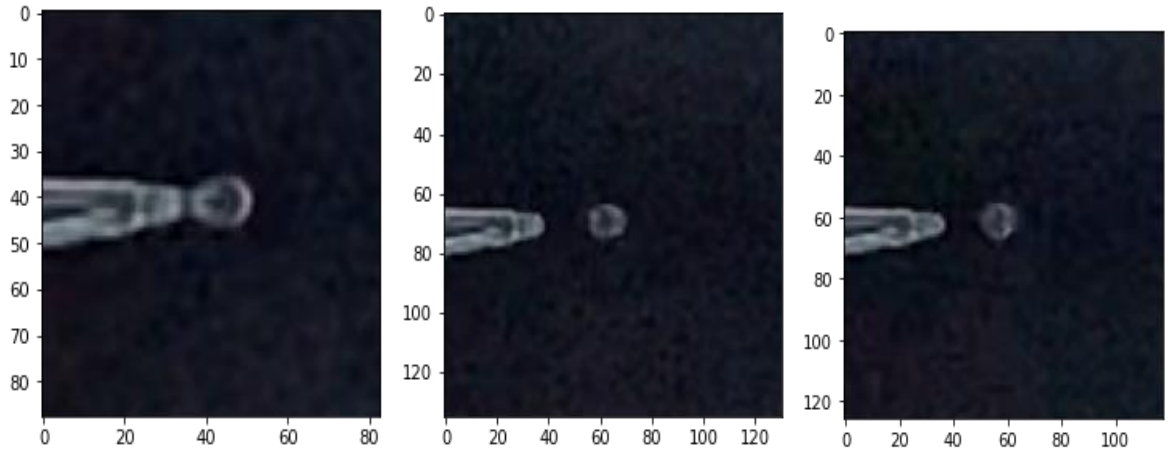

Figure 5.2: Water droplet shape change close to the burette tip.

Close to the tip, where the droplet has just been released, it is most likely oblongated (egg-shaped). The droplet is oscillating until it has a spherical shape; as shown in Figure 5.2, the frames were extracted from the Python OpenCV lab (Check Appendix C.3). Therefore, an initial determination is not caused by air-drag force; it is only interfacial tension driven oscillation.

As it falls down, velocity increases, v = 2.01 at 21cm distance from the tip (Appendix A - droplet speed); after that, the camera was not able to capture droplet the shape.

5.4 Summary of Results and Errors

5.4.1 Results and Errors of the Drop Weight Measurement

Table 5.3: Results of surface tension at 25 °C

System	Surface tension x 10^{-3} N/m		|Lit. – Exp.|/Lit x 100
	Literature	Experiment	**%**
Water	71.87	70.67	1.66
1-Butanol	23.48	23.93	1.92
Glycerol	64.00	64.9.	1.40

Table 5.3 shows a summary of the principal values obtained after performing the calculation of surface tension. It can be observed that the smallest error is 1.40 % obtained from the experiment with glycerol and the largest error is 1.92 % obtained from the experiment performed with 1-butanol. There are several effects that could cause this error. In the following lines, some possible reasons are explained:

The $r/V^{1/3}$ ratio was in the 0.36 - 0.50 range in the experiment; however, when the ratio is between 0.6 and 1, as shown in Figure 3.3, the range of the correction factor values is minimal. Furthermore, this might slight effect on the accuracy of the correction factor.

The evaporation effect may cause errors for fluids such as 1-butanol. A specific time was required for each droplet detachment to avoid hydrodynamic effects, butanol-1 was evaporated within a particular waiting time. However, the number was 1.66 %, explaining the fact that the highest error was detected for this fluid sample.

The experiments were carried out under a light source that, according to the analysis it caused some temperature increase. Even though this increase was not significant, it definitely introduced some error in the calculated values of surface tension.

Moreover, the scale had 0.01g readability which could diminish the accuracy as the surface tension is proportional directly to the mass of the liquid.

For the second attempt to calculate the surface tension by averaging droplet size from the pictures, the error was significantly high, as shown the table 5.2. There are many reasons for that; first and foremost, when acquiring the size droplet from pixel resolution, the area of interest(droplet) is slightly smaller than that chosen rectangle on the picture Figure 4.1.1. This slight difference can have a significant accuracy error. Moreover, hydrodynamic effects are also inevitable. Further investigations are needed in order to decrease the error.

While analyzing error, an interesting factor was noticed, as shown in Figure 5.3; as the fluid density increases, the error of the measurement decreases. It can be explained by the idea that as the droplet was denser, it has fewer hydrodynamic effects, and it increases the accuracy of the measurements. Further investigation needed.

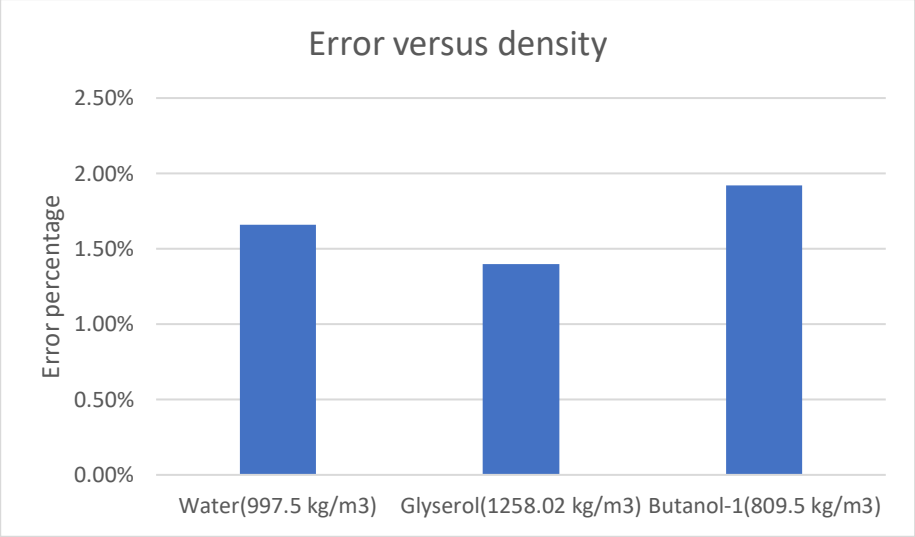

Figure 5.3: Error comparison versus sample density

Chapter 6 Conclusion

The surface tension was successfully measured by the use of the Drop Weight Method. The fast data recording and images played an essential role in the achievement of the objectives. Three different fluids were, used including distilled water, and the results obtained doesn't show a large deviation from the theoretical values found in the literature. All the efforts in order to have results as close as possible to the real ones were effective with errors no larger than 1.92%. The relation between fluid density and error was detected, which needs further deduction. Because of the time lack of time, only Newtonian fluids were used as a sample; for future work Drop Weight Method can be applied for non-Newtonian fluids to measure surface tension.

A large part of the time invested in this thesis was to build the setup. Many components were tested to meet the requirements for the experiment. The relation between deformation and fluid parameters such as density and viscosity were studied to analyse the air drag forces and the droplet shape during the fall. However, it is more comprehensive to analyze air drag fore and droplet shape changes on a large scale. Better technical equipment such as very high-resolution cameras is needed for that purpose.

It is essential to be aware of all the variables that can affect the final results because any deviation from the theory can carry some errors. During the experiment, I tried to have the conditions as close as possible to what the theory says. Despite this, some deviations were analyzed, and their impact on the calculations reduced to have accurate values. However, it is impossible to consider all the variables that can affect the final results and the error introduced by this was just accepted. For further studies, it is recommended to consider all the work done in this thesis to minimize the amount of error and increase the accuracy of the calculations.

Using the Python OpenCV library in the image processing from the slow-motion camera, pictures demonstrate to be a helpful tool to obtain droplet measurements when the droplet is moving through the air and visualize how droplets are formed. These images were linked to perform a complete analysis of what is happening during the fall. However, it was not possible to capture the droplet near the container (where velocity was high); a camera with higher magnification could be a solution. A particular phenomenon was observed when the droplet detaches from the tip of the burette t: the liquid rises rapidly inside the small tube. By

performing a specific analysis of this singularity, some other fluid properties could be inferred. The scope of the present thesis does not consider this analysis but establish some basis for further work by studying this elastic effect.

References

[1] “MIT18_357F10_Lecture2.pdf.” Accessed: Jun. 09, 2021. [Online]. Available: https://ocw.mit.edu/courses/mathematics/18-357-interfacial-phenomena-fall-2010/lecture-notes/MIT18_357F10_Lecture2.pdf

[2] M. E. M. S. and P. B. A., “Fluid Dynamics Is the Study of the Movements of Liquids and Gases,” ThoughtCo. https://www.thoughtco.com/what-is-fluid-dynamics-4019111 (accessed May 11, 2021).

[3] “What is Fluid Dynamics?” VEDANTU. https://www.vedantu.com/physics/what-is-fluid-dynamics (accessed May 11, 2021).

[4] E. Stauffer, J. A. Dolan, and R. Newman, “CHAPTER 4 - Chemistry and Physics of Fire and Liquid Fuels,” in Fire Debris Analysis, E. Stauffer, J. A. Dolan, and R. Newman, Eds. Burlington: Academic Press, 2008, pp. 85–129. doi: 10.1016/B978-012663971-1.50008-7.

[5] Z.-X. Zhang, “Chapter 5 - Effect of Temperature on Rock Fracture,” in Rock Fracture and Blasting, Z.-X. Zhang, Ed. Butterworth-Heinemann, 2016, pp. 111–133. doi: 10.1016/B978-0-12-802688-5.00005-1.

[6] K. M. Stewart, “Physical Properties of Water,” in Encyclopedia of Inland Waters, G. E. Likens, Ed. Oxford: Academic Press, 2009, pp. 148–154. doi: 10.1016/B978-012370626-3.00007-7.

[7] “Surface tension - Wikiwand.” https://www.wikiwand.com/simple/Surface_tension (accessed Jun. 01, 2021).

[8] Z.-X. Zhang, “Chapter 5 - Effect of Temperature on Rock Fracture,” in Rock Fracture and Blasting, Z.-X. Zhang, Ed. Butterworth-Heinemann, 2016, pp. 111–133. doi: 10.1016/B978-0-12-802688-5.00005-1.

[9] Rune Time, “Lecture notes from PET505 - Directional Drilling and Well Flow Engineering.,” Stavanger: University of Stavanger.

[10] J. R. Fanchi, “Chapter 7 - Measures of Rock-Fluid Interactions,” in Shared Earth Modeling, J. R. Fanchi, Ed. Woburn: Butterworth-Heinemann, 2002, pp. 108–132. doi: 10.1016/B978-075067522-2/50007-0.

[11] J. G. Speight, “Chapter 5 - Properties of Organic Compounds,” in Environmental Organic Chemistry for Engineers, J. G. Speight, Ed. Butterworth-Heinemann, 2017, pp. 203–261. doi: 10.1016/B978-0-12-804492-6.00005-8.

[12] “Interfacial Tension - an overview | ScienceDirect Topics.” https://www.sciencedirect.com/topics/engineering/interfacial-tension (accessed May 11, 2021).

[13] J. G. Speight, “Chapter 4 - Test Methods for Asphalt Binders,” in Asphalt Materials Science and Technology, J. G. Speight, Ed. Boston: Butterworth-Heinemann, 2016, pp. 137–203. doi: 10.1016/B978-0-12-800273-5.00004-0.

[14] “Interfacial Phenomena,” MIT OpenCourseWare. https://ocw.mit.edu/courses/mathematics/18-357-interfacial-phenomena-fall-2010/ (accessed Jun. 09, 2021).

[15] S. Laurén, “Surface tension measurement by Du Noüy ring method.” https://www.biolinscientific.com/blog/surface-tension-measurement-by-du-noüy-ring-method (accessed Jun. 01, 2021).

[16] “Interfacial tension.” https://www.kruss-scientific.com/en/know-how/glossary/interfacial-tension (accessed Jun. 04, 2021).

[17] J. Botchu, M. Varma, and S. Baek, Comparative Study of Rheological Properties of Ethanol and UDMH based Gel Propellants. 2013.

[18] A. Yahia, S. Mantellato, and R. J. Flatt, “7 - Concrete rheology: A basis for understanding chemical admixtures,” in Science and Technology of Concrete Admixtures, P.-C. Aïtcin and R. J. Flatt, Eds. Woodhead Publishing, 2016, pp. 97–127. doi: 10.1016/B978-0-08-100693-1.00007-2.

[19] R. Cross and C. Lindsey, “Measuring the Drag Force on a Falling Ball,” Phys. Teach., vol. 52, Feb. 2014, doi: 10.1119/1.4865522.

[20] F. Pierson and S. Whitaker, “Studies of the Drop-Weight Method for Surfactant Solutions I. Mathematical Analysis of the Adsorption of Surfactants at the Surface of a Growing Drop,” Colloids Surf. Physicochem. Eng. Asp., vol. 54, pp. 203–218, Feb. 1976, doi: 10.1016/0021-9797(76)90301-5.

[21] V. B. Fainerman and R. Miller, “2. Thermodynamics of adsorption of surfactants at the fluid interfaces,” in Studies in Interface Science, vol. 13, Elsevier, 2001, pp. 99–188. doi: 10.1016/S1383-7303(01)80063-6.

[22] J. Permprasert and S. Devahastin, “Evaluation of the effects of some additives and pH on surface tension of aqueous solutions using a drop-weight method,” J. Food Eng. - J FOOD ENG, vol. 70, pp. 219–226, Sep. 2005, doi: 10.1016/j.jfoodeng.2004.08.045.

[23] M. Hoorfar and A. W. Neumann, “Recent progress in Axisymmetric Drop Shape Analysis (ADSA),” Adv. Colloid Interface Sci., vol. 121, no. 1, pp. 25–49, Sep. 2006, doi: 10.1016/j.cis.2006.06.001.

[24] B.-B. Lee, P. Ravindra, and E.-S. Chan, “A Critical Review: Surface and Interfacial Tension Measurement by the Drop Weight Method,” Chem. Eng. Commun., vol. 195, no. 8, pp. 889–924, Apr. 2008, doi: 10.1080/00986440801905056.

[25] O. Yildirim and O. Basaran, An improved drop-weight method for measuring surface tension. 2000.

[26] J.-R. Riba and B. Esteban, “A simple laboratory experiment to measure the surface tension of a liquid in contact with air,” Eur. J. Phys., vol. 35, p. 055003, Jun. 2014, doi: 10.1088/0143-0807/35/5/055003.

[27] Earnshaw, Johnson, Carroll, and Doyle, “The Drop Volume Method for Interfacial Tension Determination: An Error Analysis.,” J. Colloid Interface Sci., 1996, doi: 10.1006/JCIS.1996.0015.

[28] M. Soni, “A simple laboratory experiment to measure the surface tension of a liquid in contact with air,” J. Pharmacogn. Phytochem., vol. 8, no. 2, pp. 2197–2202, 2019.

[29] “850 Universal Interface • UI-5000,” PASCO scientific. https://www.pasco.com/products/interfaces-and-dataloggers/ui-5000 (accessed Jun. 14, 2021).

[30] “Wireless Smart Gate • PS-3225,” PASCO scientific. https://www.pasco.com/products/sensors/wireless/ps-3225 (accessed May 31, 2021).

[31] “Smart Gate • PS-2180,” PASCO scientific. https://www.pasco.com/products/sensors/pasport/ps-2180 (accessed May 31, 2021).

[32] “AirLink Interface - PS-3200 - Products | PASCO.” https://www.pasco.com/products/interfaces-and-dataloggers/ps-3200 (accessed May 31, 2021).

[33] “Scout® SKX Electronic Balance, SKX422 AM.” https://us.ohaus.com/en-US/Products/Balances-Scales/Portable-Balances/Scout-SKX/SKX422-AM (accessed Jun. 01, 2021).

[34] R. S. Volkov, G. V. Kuznetsov, P. A. Kuibin, and P. A. Strizhak, “The ranges of the aerodynamic drag coefficient of water droplets moving through typical gas media,” J. Eng. Thermophys., vol. 25, no. 1, pp. 32–44, Jan. 2016, doi: 10.1134/S1810232816010045.

Appendix

This appendix includes the picture of the setup, different tests done on PASCO, and python scripts for splitting the slow-motion video frames, measuring the droplet size by pixel resolutions, and drop shape analyze by other pixel resolutions.

Appendix A Experimental Setup in the Mezzanine

This is the setup of the experiment done at the Mezzanine.

Appendix B Experimental Results on PASCO

This part is the results from water experiment : numbers were used for the surface tension measurements.Such as how many droplets , and the average weight.

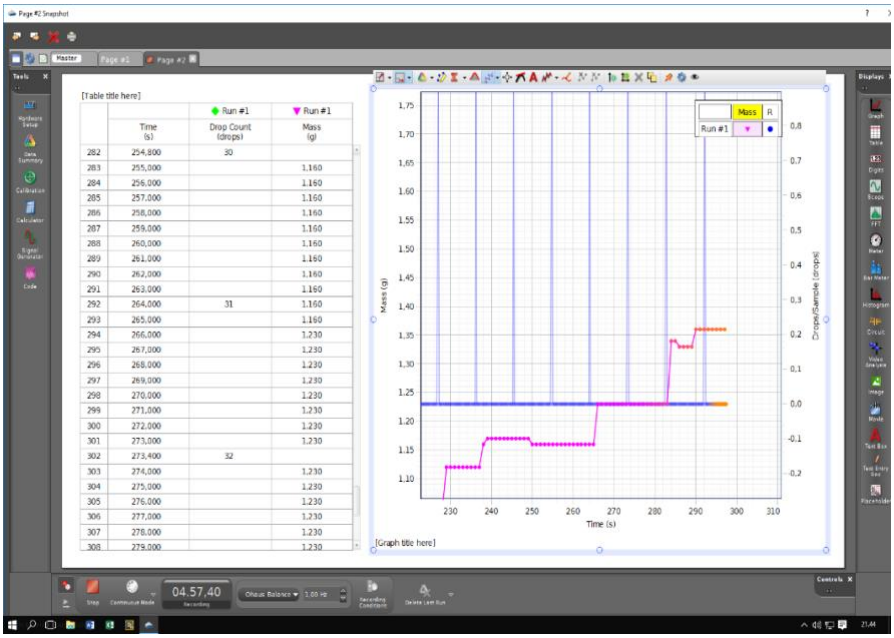

This part shows the results from glycerolexperiment : numbers were used for the surface tension measurements.

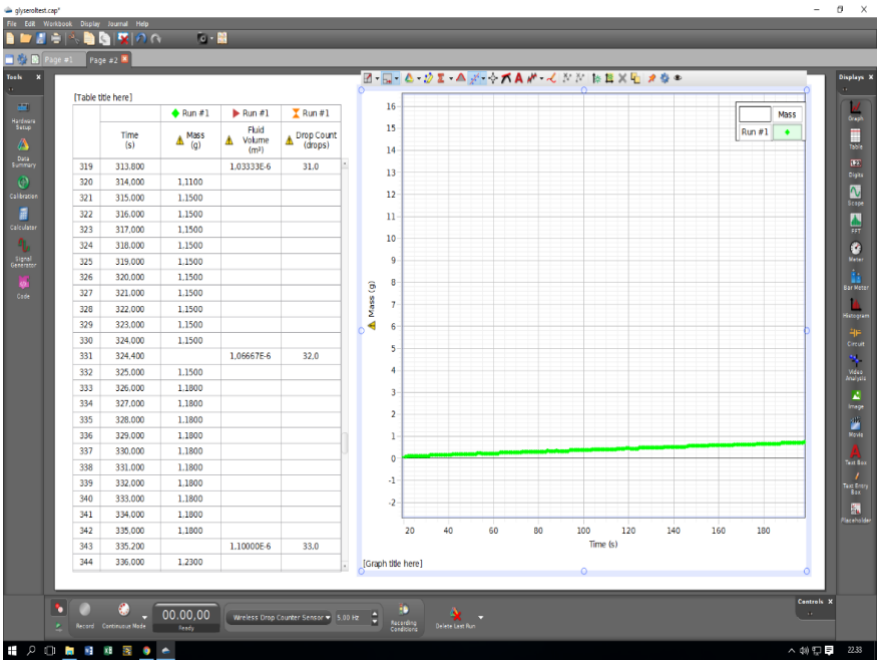

This part shows the results from 1- butanol experiment : numbers were used for the surface tension measurements.

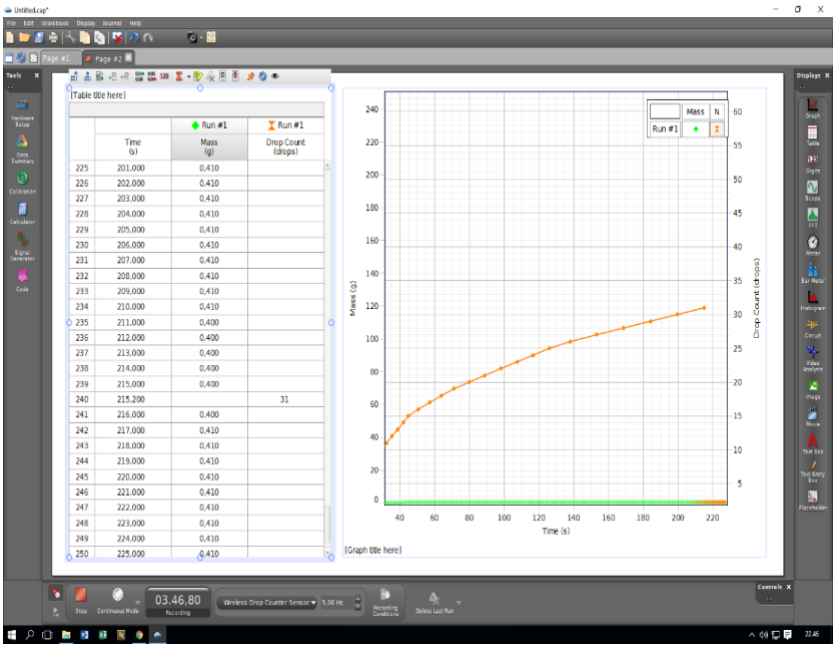

The picture below shows the velocites of the droplet at 21 cm and 11.5 cm from the surface of the sacle. They were measured by the smart gate PS2180 and the wireless smart gate 854-764.

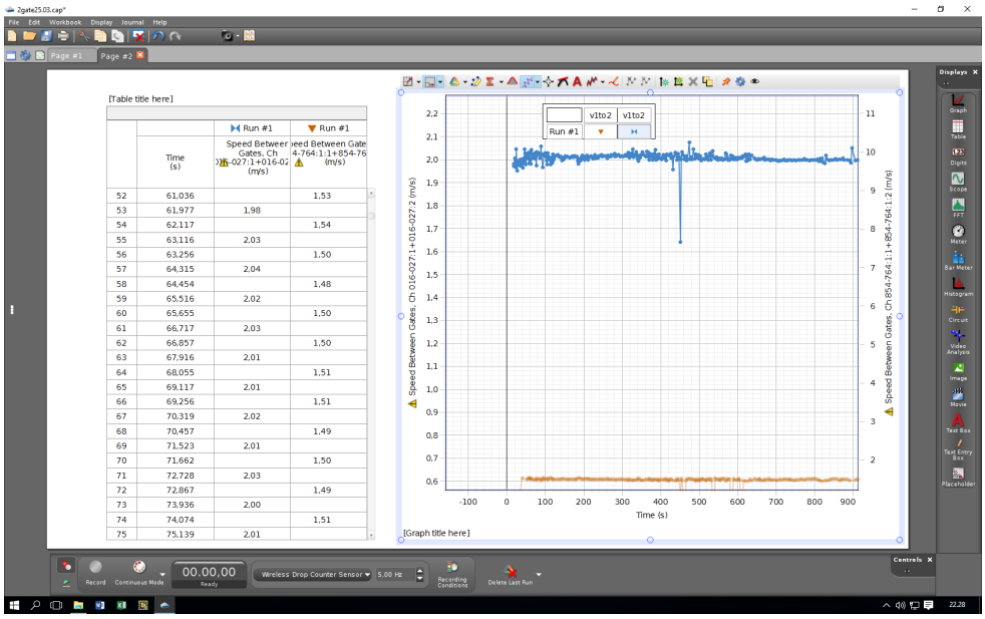

Appendix C Code Scripts

C.1 Image Processing: Video Split

[1]:
```
import cv2

cap = cv2.VideoCapture("IMG_1380.MOV")

count = 0

while cap.isOpened():

    ret, frame = cap.read()

    if ret:
        cv2.imwrite('frame{:d}.jpg'.format(count), frame)
        count += 100 # i.e. at 30 fps, this advances one second
        cap.set(1, count)
    else:
        cap.release()
        break
```

C.2 Droplet Diameter Measurement by Pixel Resolution

[40]:
```
import cv2
import matplotlib.pyplot as plt
```

[41]:
```
img = cv2.imread('frame74400.jpg')
#plt.imshow(img[600:635,955:993])
plt.imshow(img)
```

[41]:
```
<matplotlib.image.AxesImage at 0x27eaf272630>
```

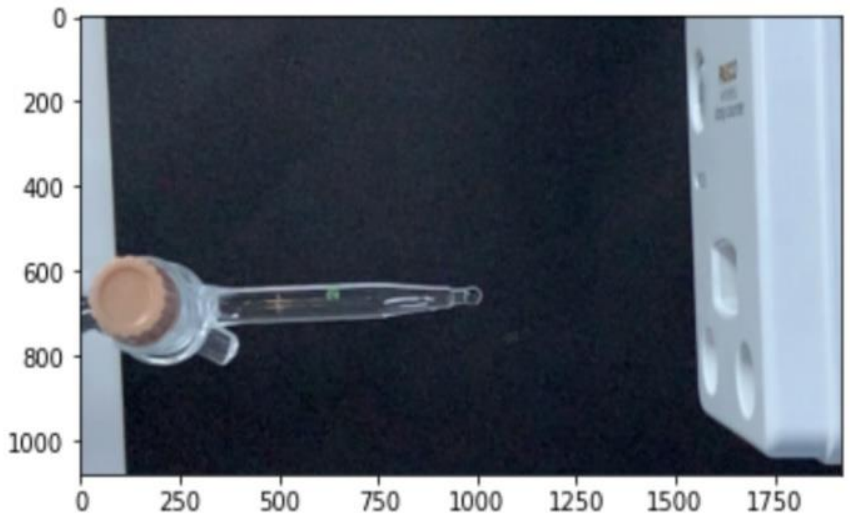

[42]:
```
roi=cv2.selectROI(img)
```

[4]:
```
roi_cropped=img[int(roi[1]):int(roi[1]+roi[3]), int(roi[0]):int(roi[0]+roi[2])]
```

[9]:
```
print('The diameter is {} mm'.format(32*0.2645833333))
```

```
The diameter is 8.4666666656 mm
```

[7]:
```
plt.imshow(roi_cropped)
print(roi_cropped.shape)
```

```
(32, 35, 3)
```

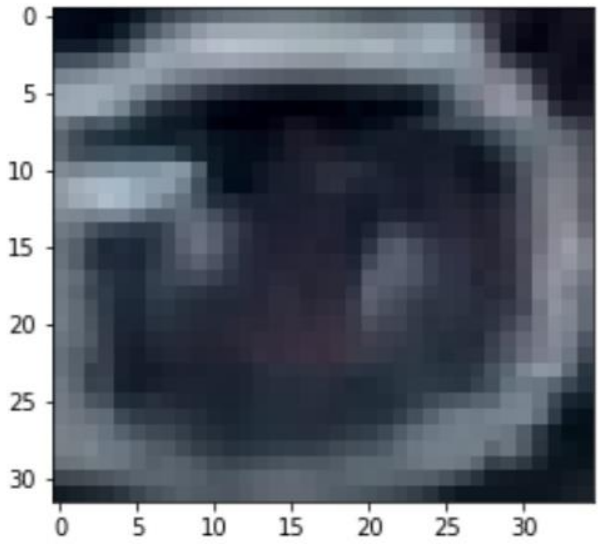

[10]:
```
print('The diameter is {} mm'.format(46*0.2645833333))
```

```
The diameter is 12.1708333318 mm
```

[6]:
```
plt.imshow(roi_cropped)
print(roi_cropped.shape)
```

```
(46, 42, 3)
```

…

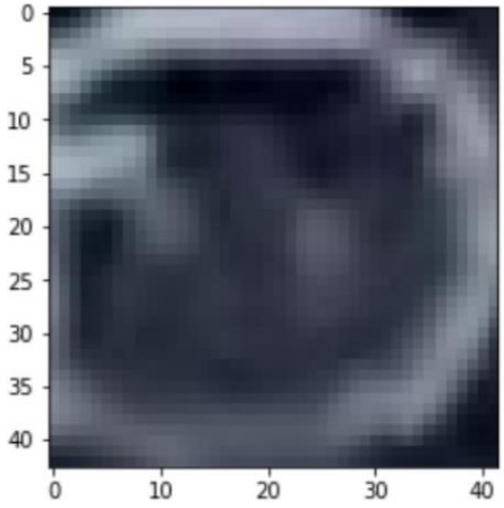

[5]:
```
print('The diameter is {} mm'.format(40*0.2645833333))
```

```
The diameter is 10.583333332 mm
```

[5]:
```
plt.imshow(roi_cropped)
print(roi_cropped.shape)
```

```
(40, 34, 3)
```

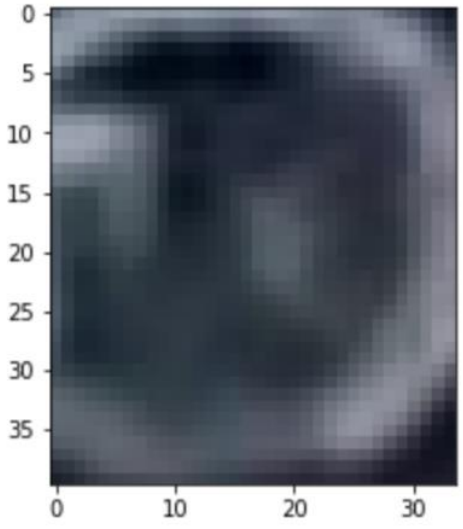

[ ]:

C.3 Droplet Shape Analyze by Splitting Frames

[1]:
```
import cv2
import matplotlib.pyplot as plt
```

[2]:
```
img = cv2.imread('frame188.jpg')
#plt.imshow(img[600:635,955:993])
plt.imshow(img)
```

[2]: <matplotlib.image.AxesImage at 0x1cd16b96438>

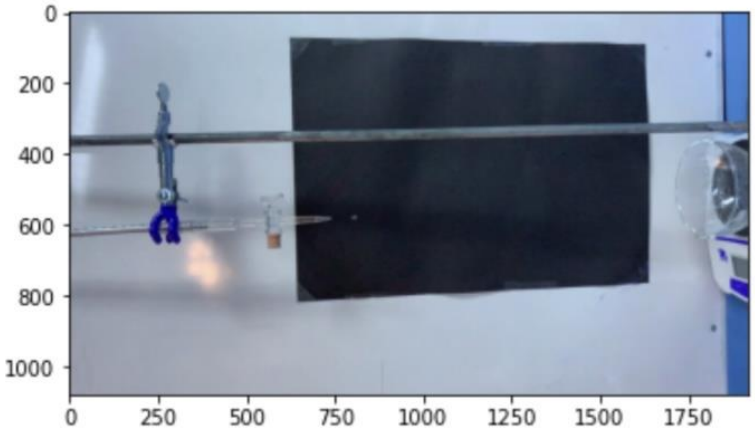

[3]:
```
roi=cv2.selectROI(img)
```

[4]:
```
roi_cropped=img[int(roi[1]):int(roi[1]+roi[3]), int(roi[0]):int(roi[0]+roi[2])]
```

[5]:
```
plt.imshow(roi_cropped)
print(roi_cropped.shape)
```

```
(88, 83, 3)
```

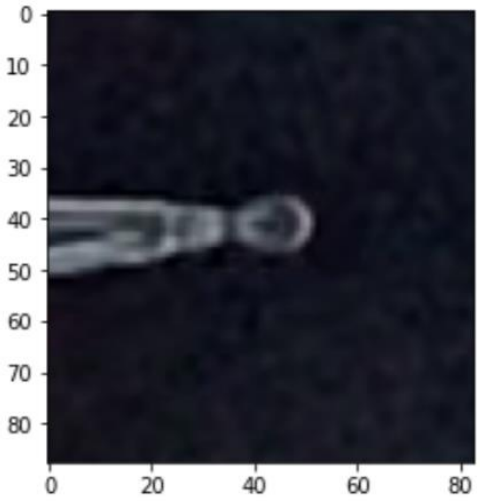

[5]:
```
plt.imshow(roi_cropped)
print(roi_cropped.shape)
```

```
(88, 81, 3)
```

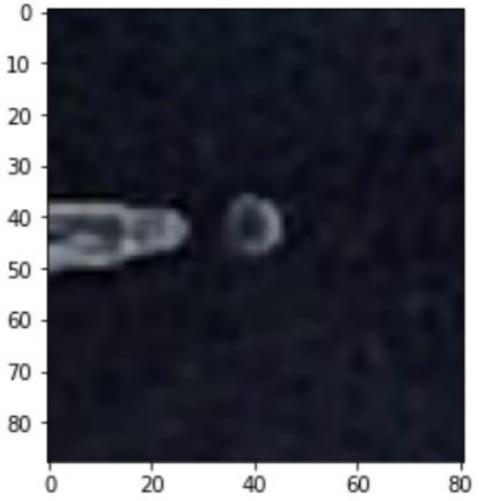

[5]:
```
plt.imshow(roi_cropped)
print(roi_cropped.shape)
```

```
(132, 121, 3)
```

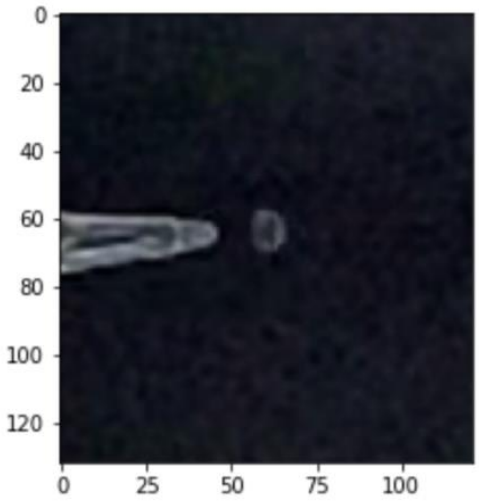

[6]:
```
plt.imshow(roi_cropped)
print(roi_cropped.shape)
```

```
(126, 118, 3)
```

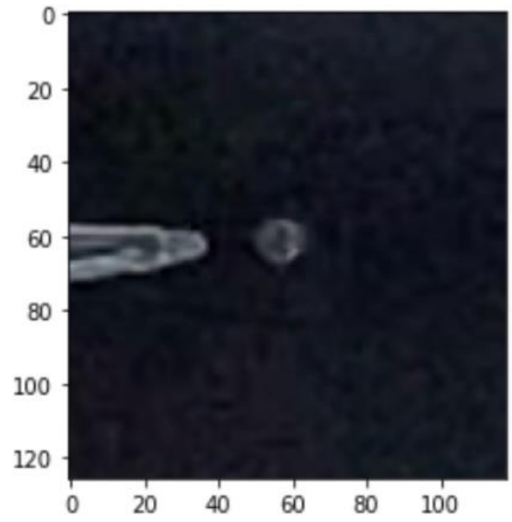

[5]:
```
plt.imshow(roi_cropped)
print(roi_cropped.shape)
```

```
(135, 131, 3)
```

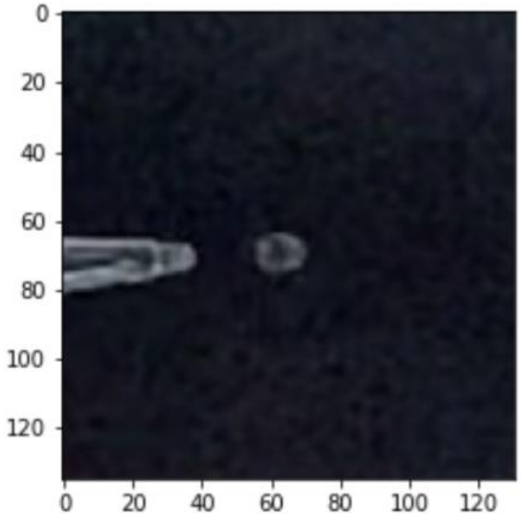

.

[5]:
```
plt.imshow(roi_cropped)
print(roi_cropped.shape)
```

```
(122, 115, 3)
```

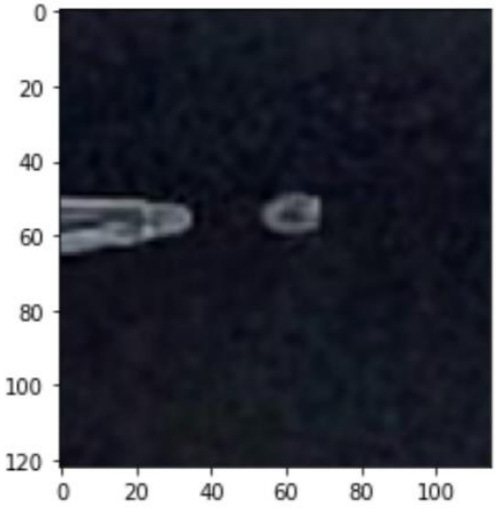

[5]:
```
plt.imshow(roi_cropped)
print(roi_cropped.shape)
```

```
(128, 124, 3)
```

...

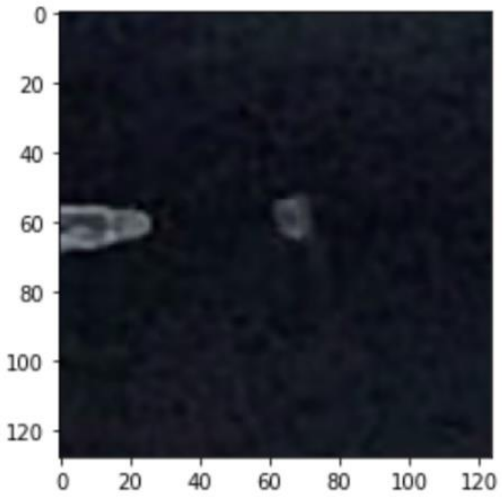
0
20
40
60
80
100
120
0
20
40
60
80
100
120

[ ]:

...

C.4 Droplet Pictures by BASLER acA800-510uc

The image below is one frame from the slow motion video where the droplet is close to the syrface and velocity is high and the shape is blurry and not identified.